Pergamon

Pattern Recognition, Vol. 30, No. 1, pp. 9–17, 1997

0031-3203/97 $17.00+.00

PII:S0031-3203(96)00063-5

OFF-LINE SIGNATURE VERIFICATION BASED ON GEOMETRIC FEATURE EXTRACTION AND NEURAL NETWORK CLASSIFICATION

KAI HUANG* and HONG YAN
Department of Electrical Engineering, University of Sydney, NSW 2006, Australia

(*Received* 25 *October* 1995; *in revised form* 26 *March* 1996; *received for publication* 15 *April* 1996)

Abstract—In this paper a method for off-line signature verification based on geometric feature extraction and neural network classification is proposed. The role of signature shape description and shape similarity measure is discussed in the context of signature recognition and verification. Geometric features of input signature image are simultaneously examined under several scales by a neural network classifier. An overall match rating is generated by combining the outputs at each scale. Artificially generated genuine and forgery samples from enrollment reference signatures are used to train the network, which allows definite training control and at the same time significantly reduces the number of enrollment samples required to achieve a good performance. Experiments show that 90% correct classification rate can be achieved on a database of over 3000 signature images. Copyright © 1996 Pattern Recognition Society. Published by Elsevier Science Ltd.

Off-line signature verification
Signature shape description and similarity measure
Signature image alignment
Neural network classifier

1. INTRODUCTION

Biometric verification is an important research area targeted at automatic identity verification applications. Current security practices usually involve the use of PIN numbers, passwords, and access cards. These tokens are not very reliable in that they can be forgotten or lost, and no further restrictions exist which can prevent an unauthorized person from using them in an automatic machine verification environment. Biometric measures, on the other hand, are not easily duplicated and cannot be lost or stolen, hence are more secure. Powerful computer technologies today can easily accommodate common biometric verification tasks, especially with the introduction of smartcards.

There are two types of biometrics: physiological, e.g. iris pattern and finger print; behavioral, e.g. speech and handwriting. Handwritten signature verification is a behavioral biometric verification, and most of us are familiar with the process of verifying a handwriting against a signature record for identification, especially in legal, banking, and other high security environments.

Automatic handwritten signature verification systems (AHSVS) are either on-line or off-line, which are differentiated by the data acquisition method.[1–3] In an on-line system, signature traces are acquired in real time with digitizing tablets, instrumented pens, or other specialized hardwares during the signing process. In an off-line system, signature images are acquired with scanners or cameras after the complete signatures have been written. Common to both types of systems are the static calligraphic information, i.e. the geometric properties of the signature. Dynamic handwriting features, such as motion, pressure, and timing information, are readily captured on-line, but not recoverable with good accuracy off-line.[1]

The complexity of signature verification lies in the variability of signing. For well-practiced signatures, interpersonal variations should be much larger than intrapersonal ones. The aim of an automatic signature verification system is to extract a set of least variable features from reference signature samples, such that the intrapersonal variations are minimized. These features are then used to form a similarity measure to classify further inputs as either genuine or forgery, based on the closeness of the match.

Most of AHSVS are on-line systems which utilize dynamic features to achieve excellent verification results.[1,4] A wide range of techniques have been applied in the past to solve the more difficult off-line signature verification problems. Elastic image matching has been successfully used by de Bruyne *et al.* to reduce random forgery acceptance rate.[5] Elastic signature envelop matching has also been used to compute distances between signatures.[6] Techniques that are traditionally developed for character recognition are also being applied to signature verification. For example, extended shadow-code has been used as a global signature shape descriptor in the elimination of random forgeries.[7]

Effective feature extraction is important in all pattern recognition tasks. Signature image analysis based on gradient operator derived features such as directional

* Author to whom correspondence should be addressed. Tel.: +61 2 351-4824; fax: +61 2 351-3847; e-mail: kai@ee.usyd.edu.au.

Probability Density Function (PDF)[8] has been investigated, and image understanding based approach has also been implemented with good results on random forgery data.[9] Analysis based on various histograms and their derivatives has been reported by Ammar, which are successful in the detection of highly skilled forgeries.[10] More recent efforts tend to utilize neural networks and multi-resolution image analysis in the classification of signature data.[4]

The role of signature shape representation and signature similarity measure derived from shape representation needs to be emphasized.[11–13] In this paper, we use the following features to describe the shape of a signature: core, outline, ink area distribution, and signature frontiers. A set of directional filters are used to segment the signature images using these features into consistent parts. A statistical model for each signature class can then be built from a few training reference samples, and a similarity measure can be set to classify genuine and forgery inputs with reasonable confidence.

The proposed method in this paper uses multi-resolution feature extraction and multiple expert voting techniques. When examining handwritten signatures, people usually perform the following steps. First the rough overall shape is compared. Then closer details such as how each stroke starts and ends, the ink trace path and other aspects of the writing are looked at individually. Finally the overall impression of authenticity is made. The current study is aimed at the first stage signature classification, which performs rough shape comparison to filter out most of the less skilled forgery inputs, simulating the above steps. Signature shape is learned by neural networks at multiple resolutions selected by experiments. A set of multi-resolution grids with fuzzified borders are overlaid on top of signature shape representations when extracting local shape features. Neural network structure is used in the construction of a statistical model at every grid resolution for each signature class. The classifier, which is the trained neural network model, is also built. Artificial genuine and forgery samples are created to train the neural network classifier by applying perturbation to a small set of genuine reference samples. The acceptance and rejection space are effectively controlled by perturbation parameters.

The rest of the paper is divided into five sections. In Section 2, the signature database used in our experiments is described. In Section 3, signature shape feature extraction and alignment are discussed. Neural network classifier training method is described in Section 4. In Section 5, system implementation and experiment results are discussed. Finally, conclusions of the study are presented in Section 6.

2. SIGNATURE DATABASE CONSTRUCTION

2.1. Signature data collection

A total of 3528 signature images are collected to form the signature database. These images belong to 21 sets of different signatures. Each set comprises one A4 page of genuine and six A4 pages of forgery signatures. They are scanned, one page at a time, at resolution of 100 dpi, 8-bit gray-scale. An A4 page is divided into 12×2 rectangles with dashed lines. Twenty-four genuine signatures are signed by a volunteer and six lots of 24 forged signatures are produced by other volunteers. Each volunteer may be asked to produce one to three other people's signatures, given photocopies of the genuine signature pages. The forgeries, either freehand or traced, encompass varying skill levels (Fig. 1).

2.2. Signature image preprocessing

The signature images are first cut out from the scanned A4 page image by a separate form processing program. The dash lines on the form are located and are used as the primary separators in the extraction of individual images. It is observed that some writers use the lower grid lines as their signature reference line, as a result part of the signature trace is cut off by the extraction program. From visual inspection, the extracted images contain most of the signature information and some loss is tolerable. It helps to force the classification system to be more robust against such situations.

Excessive white area in each image is trimmed off, and the signature is centered at gray-level centroid by adding clean border areas to make it more pleasing to the eye. Standard noise reduction and isolated peak noise removal techniques, such as median-filtering and average filtering,[15] are used to clean the initial image. A binarized signature mask is obtained by thresholding followed by morphological operations[15] to fill small holes and to remove small connected components mostly generated by noisy background. It is used to mask out the gray-leveled version of the clean, centered signature image S_{gray} (Fig. 2).

3. EXTRACTION AND ALIGNMENT OF SIGNATURE SHAPE FEATURES

3.1. Feature extraction

For a signature image S_{gray} of width w and height h, let P be a pixel inside S_{gray}. The position of P is denoted by (i, j), where $0<i<w-1$ and $0<j<h-1$, and the gray level value of P is denoted by g_P, where $g_P=S_{gray}(i, j)$. The maximum and minimum gray-level values of S_{gray} are denoted by g_{max} and g_{min} respectively, where $g_{max}=\max S_{gray}(i, j)$, and $g_{min}=\min S_{gray}(i, j)$, for all i and j. The neighbors of pixel P are defined by a 3×3 window

P_2	P_1	P_0
P_3	P	P_7
P_4	P_5	P_6

or

NW	N	NE
W	P	E
SW	S	SE

3.1.1. Shape features from signature image. The following shape features are extracted from signature images:

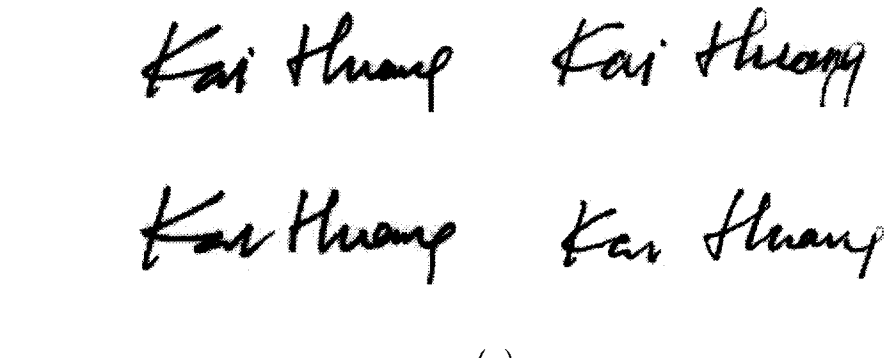

(a)

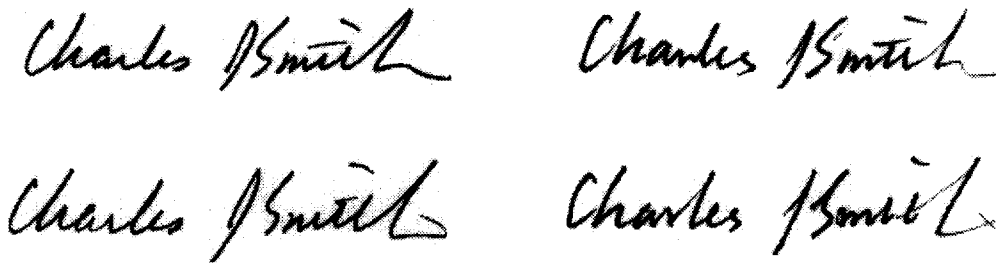

(b)

(c)

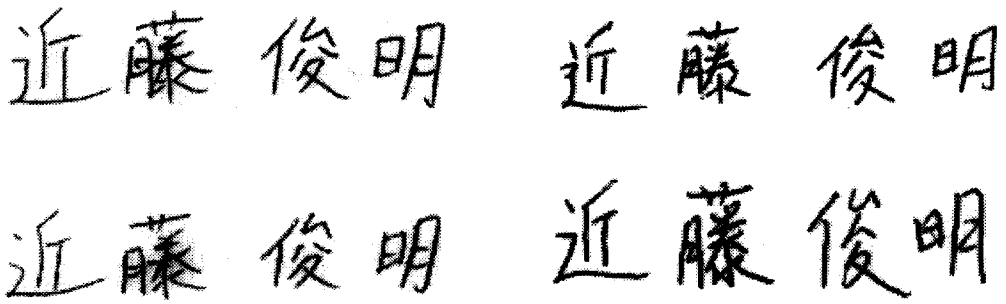

(d)

Fig. 1. Examples of genuine and forgery signatures. Genuine samples are on the left, and forgery samples are on the right. The forged signatures are either simple freehand, skilled freehand or traced. (a) and (b) show common cursive type signature samples and forgeries, (c) shows graphical type signatures, and (d) shows oriental type signatures.

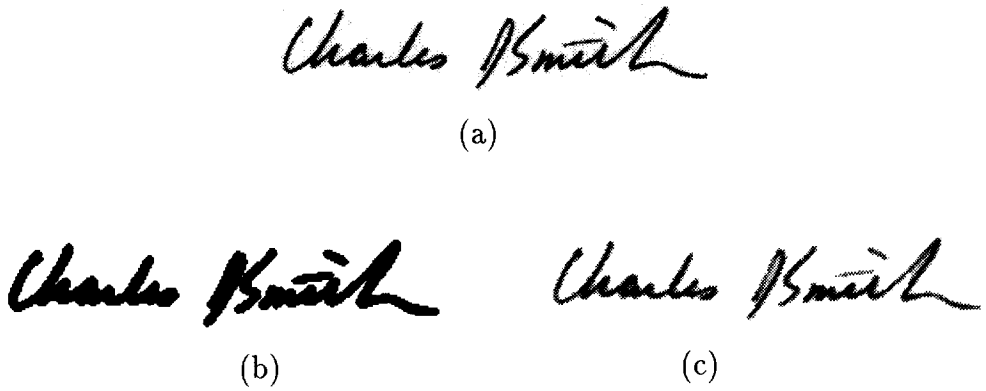

(a) (b) (c)

Fig. 2. Preprocessing of signature image. (a) is the signature cut-out from form, (b) is the binarized mask, and (c) is the cleaned image after processing.

- Core feature F_{core}:

Signature core is defined as the skeleton of the pen trace. The core feature is a useful structural representation of a signature. In conjunction with other features, it is possible to extract dominant and individual pen strokes. It is also invariant with respect to pen trace thickness. Strict single pixel connectivity is not critical in our current application. Instead of applying standard skeletonizing algorithm on binarized image, the core feature is extracted directly from the gray-level image using a 3×3 operator, to preserve the original structure as closely as possible. A pixel is core if its gray-level value is a local peak (Fig. 3a):

$$P \in F_{\text{core}}, \quad \text{if} \sum_{k=0}^{7} step(g_P \geq g_{P_k}) \leq 6,$$

where

$$step(g_P \geq g_{P_k}) = \begin{cases} 1 & \text{if } g_P \geq g_{P_k}, \\ 0 & \text{otherwise.} \end{cases} \tag{1}$$

- Signature outline F_{outline}:

The outline feature contains most of the shape information. It is extracted from the gray-level image after thresholding, again using a 3×3 operator. A threshold θ_{outline} is set to be 25% mark in the range of maximum and minimum gray-level intensities in the image, then pixels whose gray-level intensity values are above the threshold and whose 8-neighbor count is below 8 must be on the outline [Fig. 3(b)]. That is,

$$\theta_{\text{outline}} = g_{\min} + 0.25(g_{\max} - g_{\min}),$$

and

$$P \in F_{\text{outline}}, \quad \text{if } (g_P > \theta_{\text{outline}}) \text{ and } (\sum_{k=0}^{7} g_{P_k} > \theta_{\text{outline}}) < 8. \tag{2}$$

- Ink distribution F_{ink}:

Several resolutions of ink distribution in the signature image are extracted, coarse [Fig. 3(c)], and fine [Fig. 3(d)]. This feature is mainly used in the alignment of two signatures. It is important that during signature alignment only the dominant parts are considered. The coarse ink distribution feature is useful for translational and linear scaling alignment, while the fine one is to be used in non-linear scaling. Coarse ink distribution feature is extracted on grid size of 8×8, and the fine one on grid size 4×4. A grid is filled if the signature image pixel count inside the grid is above 50% of the total pixels inside the grid.

- High pressure region feature F_{hpr}:

High pressure feature has been used by Ammar *et al.*[14] to detect skilled forgeries. It is extracted to indicate regions where more emphasis has been made by the signer, usually the darker area in the scanned image. A threshold θ_{hpr} is set to be 75% mark between maximum and minimum gray-level intensities. Pixels of gray-level intensity values larger than threshold are considered belonging to high pressure regions [Fig. 3(e)].

$$\theta_{\text{hpr}} = g_{\min} + 0.75(g_{\max} - g_{\min}),$$

and

$$P \in F_{\text{hpr}}, \quad \text{if} g_P > \theta_{\text{hpr}}. \tag{3}$$

- Directional frontiers features F_{frs}:

These features contain directional information as well as signature outline segmentation information individually, and pen stroke width variation information when combined. A pixel is a signature north frontier if its north neighbor is background, for example. North, south, east, west, north-east, north-west, south-east, and south-west directional frontiers are extracted [Fig. 3(f)–(m)].

3.1.2. Global geometric features. The following global geometric features are also extracted, by analyzing feature projections and connected feature components:

- area of feature pixels in core, outline, high pressure region, directional frontiers, coarse, and fine ink distribution,
- number of constituent parts in signature as determined from coarse and fine ink distribution,
- the centroid location, and width and height of each signature constituent parts, and

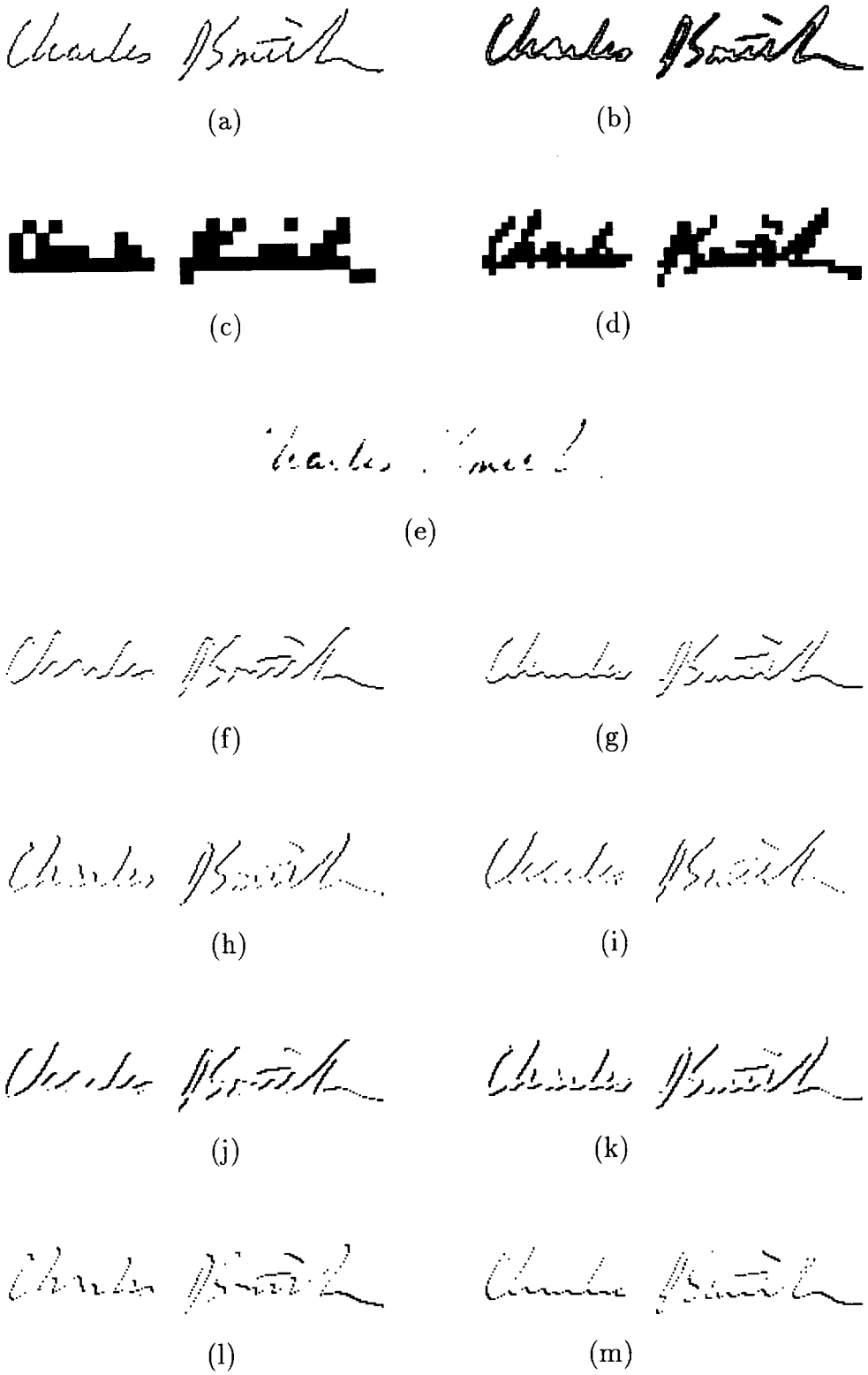

Fig. 3. Feature images extracted from a signature: (a) core, (b) signature outline, (c) coarse resolution ink distribution, (d) fine resolution ink distribution, (e) high pressure region feature, and (f)–(m) directional frontiers.

• the dynamic warping distance to reference template computed during feature alignment, to be described later in Section 3.2.

3.1.3. Local shape features. A set of rectangular grids are overlaid on top of each signature shape representation when extracting features. A coarse grid of size 3×10 is used as the basis structure (Fig. 4). Using the coarse grid, the image is divided into three horizontal zones roughly corresponding to upper, middle, and lower zones of the writing, and into ten vertical zones with width of an average lower-case letter. The highest resolution grid is 6×20. A medium grid of size 4×15 is also used. The borders of these grids are fuzzified to reduce the effect of abrupt changes on feature matching if severe misalignment occurs. The extent of fuzzy region is determined by a percentage factor p_f, where $0<p_f<1$. The horizontal extent equals the width of grid box W_g multiplied by p_f, and the vertical extent equals the height of grid box H_g multiplied by p_f. During our experiment, the value of p_f is set to 0.15. Inside each grid, the number of feature pixels are counted. For feature pixels near boundary regions, a linear fuzzy weighting factor is multiplied. The feature value is then normalized by the perimeter value of the grid box.

The following directional filters are applied to core, outline features, and frontier features when these features are individually used as signature shape representation:

$$\begin{bmatrix}1&1\\0&0\end{bmatrix},\ \begin{bmatrix}1&0\\1&0\end{bmatrix},\ \begin{bmatrix}1&0\\0&1\end{bmatrix},\ \begin{bmatrix}0&1\\1&0\end{bmatrix}.$$

Other common feature vector construction techniques found mostly in character recognition works, such as curvature estimation at each feature point, can also be considered.

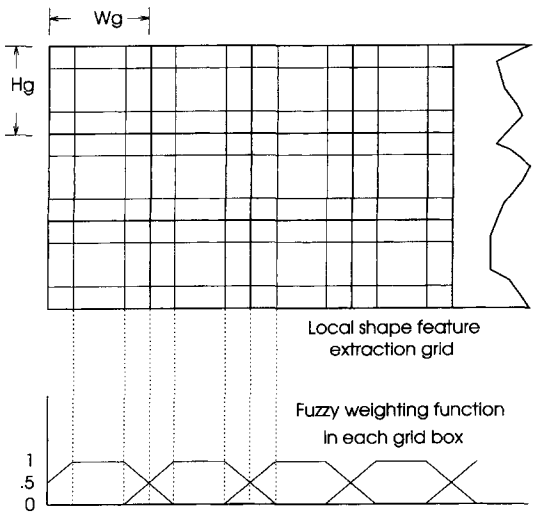

Fig. 4. Local shape feature extraction grid with fuzzified border regions. The regular grid location is indicated by thick border line. The extent of fuzzy region is indicated by thin border line. The linear fuzzy weighting scheme is illustrated in the lower part.

3.2. Feature alignment

To effectively reduce intrapersonal variations, the set of reference signatures as well as input test signatures need to be carefully aligned before local shape feature extraction and statistical model construction or verification. This is an area which has not been well documented in the past.

The horizontal and vertical projections of the binarized ink area image are obtained for all reference samples belonging to the same signature. One set of projections are selected arbitrarily as a common reference template, and projections from other reference samples are transformed against the template to find the function which maximizes correlation, hence to register these signature samples in a better way.

The transformation functions considered are linear translation, scaling, and non-linear scaling by elastic matching. On the coarse ink area level, linear translations of signature constituent parts are performed. This step is necessary since from observations of many genuine signatures consisting of multiple parts, the lengths of white space separating these parts are unexpectedly variable. Linear scaling is performed in feature space by applying fixed size grids on different size feature images during local feature extraction, rather than scaling in image space to reduce distortions.

More detailed signature image registration is performed by non-linear scaling. A two-dimensional surface scaling function is searched by elastic matching of the horizontal and vertical projections of the fine resolution ink area image against those from the common template using a dynamic programming based technique.[16] The accumulated warping distance is utilized as a global feature when non-linear scaling is performed. The non-linear scaling method, which itself can serve as a signature classifier, is the subject of a separate paper.

4. TRAINING THE NEURAL NETWORK CLASSIFIER

Signature verification is a problem in which we can neither completely specify the true sample space nor the false one. Neural network is proven to be robust and flexible in many applications. It has the ability to generalize its solution space by interpolation and extrapolation. If trained adequately, accurate and meaningful results can be obtained from a neural network classifier when previously unseen samples are applied. A person could sign his or her signature in three or more styles, with some styles occurring more frequently than others. Currently we hope that a generalized neural network can be trained to cover all these varying styles. Multi-layer perceptron is selected as the structure for the signature classifier.

4.1. Perturbation sample generation

To model practical situations, a small set of reference samples from the genuine signature set and artificially generated samples from these references are used as training data. Slightly perturbed versions of genuine signatures are used as genuine training samples. Heavily distorted versions are used as forgery training samples. The perturbations and their corresponding parameters are slant distortion θ_{slant}, size distortion S_x and S_y for scaling in horizontal and vertical directions, rotation distortion θ_{rotate} and perspective view distortion λ. Consider the writing process where the writer may hold the pen at slightly different positions and slant angles each time the signature is reproduced, size, slant and perspective variations are naturally added to the pen trace image. Hence it is useful to allow such kinds of small perturbations.

The gray-level image itself is distorted when generating artificial training samples. The centroid location of each signature image under perturbation remains invariant. Pixel coordinates in the distorted image rectangle are reverse mapped to the original image space under perturbation equations, then the gray-level value of the pixel is determined by bi-linear interpolation.[15] Table 1 shows the reverse mapping equations and Table 2 shows the values of perturbation parameters chosen during experiment.

4.2. Neural network training

The multi-layer perceptron network is trained with 8 enrolled reference samples and 320 or so derived samples as genuine training data, 640 derived samples plus random samples, derived data from other signature classes (total 3000) as forgery training data. The trained network should draw a clear boundary for the trained genuines and the rest should be forgery space.

5. SYSTEM IMPLEMENTATION AND RESULTS

Individual signature verifier is constructed for each enrolled signature class. Additional user enrollment will not affect the existing trained system. Each verifier consists of several simple three-layer perceptron networks, one network per feature resolution plus a decision network whose function is to combine the responses from feature networks and to produce a final confidence rating (Fig. 5).

For feature networks, the number of inputs equals the feature vector size, which is determined from the feature resolution. The number of units in the single hidden layer is determined from experiment such that the network will train adequately. It is chosen to be 20. There are two output units, corresponding to true and false response nodes. The decision network takes outputs from all feature networks and it has an input layer of size 6, one hidden layer of size 6, and a single output.

The system flow diagram is illustrated in Fig. 6. During training phase, eight genuine reference samples and derived data from them are applied to the feature networks under supervised learning. The three feature networks in each verifier are trained individually. The responses from feature networks are recorded and applied to the decision network, again under supervised learning. The signature statistical model as well as the discriminant measure are stored in the network connection weights. Global features are collected but not currently utilized.

Once trained, the verifier performance is evaluated for both random forgeries and targeted forgeries. All genuine signatures and all forgery signatures are used as testing data. Under random forgery test, all data sets except the one with identification number the same as the verifier are applied. The average false acceptance rate for each signature class is just below 0.05%, for a test set size of 3360 samples. Under targeted forgery test, the test size is 24 genuine samples and 144 forgery samples, the average correct classification rate is about 90% when no data rejection is allowed (Table 3).

6. CONCLUSIONS

An off-line signature verification method based on geometric feature extraction of localized, aligned shape

Table 1. Reverse mapping equations for all perturbation operations in artificial training sample generation. (x, y) is the co-ordinate of a pixel in the distorted image, and (x', y') is the corresponding co-ordinate location in the original image

Pertubation	Reverse –mapping equation	
Slant	$x'=x-y\tan\theta_{\text{slant}}$,	$y'=y$
Rotation	$x'=x\cos\theta_{\text{rotate}}-y\sin\theta_{\text{rotate}}$	$y'=y\cos\theta_{\text{rotate}}+x\sin\theta_{\text{rotate}}$
Scaling	$x'=x/S_x$	$y'=y/S_y$
Perspective	$x'=x\lambda/(\lambda-5)$,	$y'=y\lambda/(\lambda-5)$

Table 2. Perturbation parameter values used in generating artificial training samples

Pertubation	Parameter	Slight distortions	Heavy distortions
Slant	θ_{slant}	0°; ±1.5°; ±3.0°	±5.0°; ±10.0°; ±20.0°
Rotation	θ_{rotate}	0°; ±1.5°; ±3.0°	±5.0°; ±10.0°; ±20.0°
Scaling	S_x	1; 1±0.05; 1±0.1	0.4; 0.5; 0.6; 0.7; 1.3; 1.4; 1.5; 1.6
Scaling	S_y	1; 1±0.05; 1±0.1	0.4; 0.5; 0.6; 0.7; 1.3; 1.4; 1.5; 1.6
Perspective	λ	±(20±1); ±(20±2);	±(10±1); ±(10±2); ±(13±1)

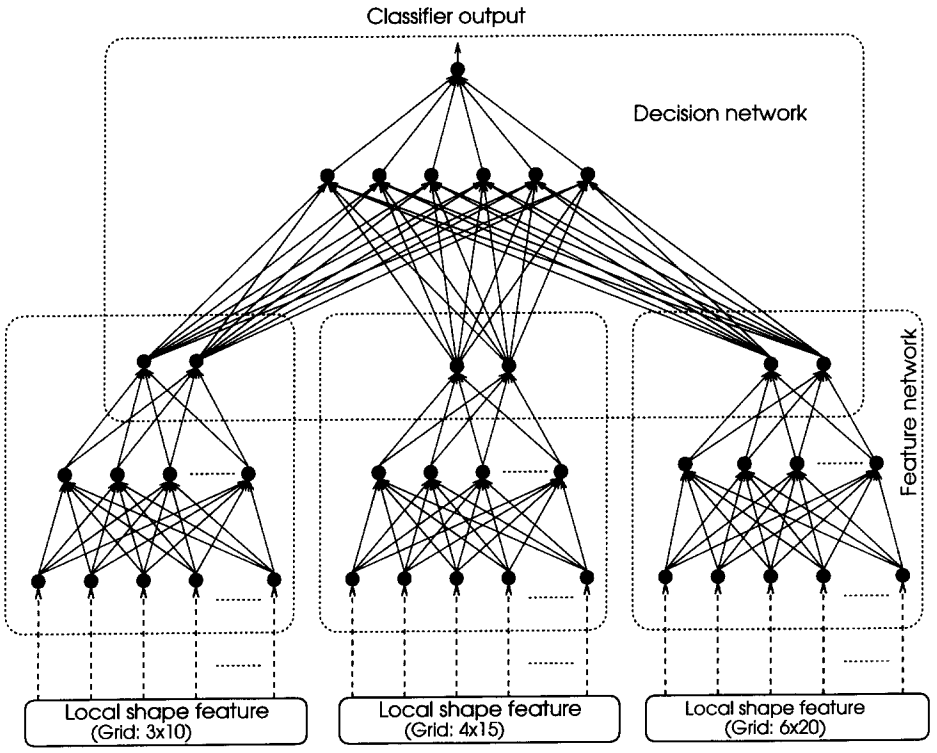

Fig. 5. Neural network classifier for signature verification. It consists of several feature networks and a decision network.

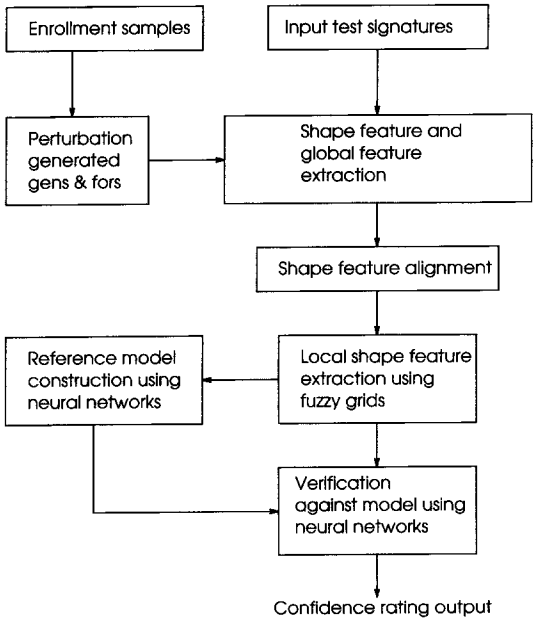

Fig. 6. Signature verification system diagram. It shows the flow path for both the training phase (left portion) and testing phase (right portion) of the system.

features and neural network classification is described and its effectiveness is evaluated on a moderate size experimental signature database. The experimental results show that the signature classifiers constructed with the proposed method are very effective in random forgery detection, however its performance is reduced when targeted forgery are applied, especially when skilled traced forgeries are involved. As a first stage verifier, it can label a suitable amount of inputs as questionables and pass them to a more detailed but time-consuming verifier, thus improves both the speed and accuracy of the complete system.

Table 3. Experimental result on signature database for targeted forgery test

Total false rejects	Total false accepts	Total genuines	Total forgeries
56	357	504	3024
Average false rejects	Average false accepts	Type I error	Type II error
3	17	11.1%	11.8%

Acknowledgements—The authors wish to thank all who have contributed to the signature database, and D. J. Ding for valuable suggestions and discussions.

REFERENCES

1. R. Plamondon and G. Lorette, Automatic signature verification and writer identification: the state of the art, *Pattern Recognition* **22**, 107–131 (1989).
2. G. Pirlo, Algorithms for signature verification, *Fundamentals in Handwriting Recognition*, S. Impedovo, ed., pp. 435–454. Springer, Berlin (1994).
3. R. Plamondon and G. Lorette, Designing an automatic signature verifier: problem definition and system descrip-

tion, *Computer Processing of Handwriting*, R. Plamondon and C. G. Leedham, eds, pp. 3–20. World Scientific, Singapore (1990).
4. F. Leclerc and R. Plamondon, Automatic signature verification: the state of the art 1989–1993, *Int. J. Pattern Recognition Artific. Intell.* **8**, 643–659 (1994).
5. P. de Bruyne and R. Forre, Signature verification with elastic image matching, *Int. Carnahan Conf. on Security Technology: Crime Countermeasures*, Gothenburg, Sweden, 113–118. University of Kentucky, Lexington, KY, U.S.A. (1986).
6. F. Nouboud, Handwritten signature verification: a global approach, *Fundamentals in Handwriting Recognition*, S. Impedovo, ed., pp. 455–459. Springer, Berlin (1994).
7. R. Sabourin, M. Cheriet and G. Genest, An extended-shadow-code based approach for off-line signature verification, *Proc. ICDAR'93: Int. Conf. on Document Analysis and Recognition*, Tsukuba Science City, Japan, 1–5. IEEE Computer Society Press (1993).
8. R. Sabourin and J. P. Drouhard, Off-line signature verification using directional PDF and neural networks, *Proc. 11th IAPR Int. Conf. on Pattern Recognition*, 321–325 (1992).
9. R. Sabourin, R. Plamondon and L. Beaumier, Structural interpretation of handwritten signature images, *Int. J. Pattern Recognition Artific. Intell.* **8**, 709–748 (1994).
10. M. Ammar, Progress in verifcation of skillfully simulated handwritten signature images, *Int. J. Pattern Recognition Artific. Intell.* **5**, 337–351 (1991).
11. S. Lee and J. C. Pan, Offline tracing and representation of signatures, *IEEE Trans. Systems Man Cybernet.* **22**, 755–771 (1992).
12. M. Ammar, Y. Yoshida and T. Fukumura, Structural description and classification of signature images, *Pattern Recognition* **23**, 697–710 (1990).
13. C. D. Lee and R. A. Abbey, *Classification and Identication of Handwriting*. D. Appleton and Company, New York (1922) .
14. M. Ammar, Y. Yoshida and T. Fukumura, A new effective approach for off-line verification of signatures by using pressure features, *Proc. 8th Int. Conf. on Pattern Recognition*, Paris, 566–569 (1986).
15. R. C. Gonzalez and R. E. Woods, *Digital Image Processing*, Addison-Wesley, Reading, Massachusetts (1992).
16. H. Sakoe and S. Chiba, Dynamic programming algorithm optimization for spoken word recognition, *IEEE Trans. Acoust. Speech Signal Process.* **ASSP-26**, 43–49 (1978).

About the Author — KAI HUANG received his B.Sc. degree in Computer Science and Pure Mathematics in 1991 and B.E. (Honors) degree in Electrical Engineering in 1993, both from the University of Sydney. He is currently a Ph.D. student in the Department of Electrical Engineering at the University of Sydney. His research interests include pattern recognition, signal and image processing and automatic handwritten signature verification.

About the Author — HONG YAN received his B.E. degree from Nanking Institute of Posts and Telecommunications in 1982, M.S.E. degree from the University of Michigan in 1984, and Ph.D. degree from Yale University in 1989, all in electrical engineering. From 1987 to 1989 he was a research scientist at General Network Corporation, New Haven, CT, U.S.A., where he worked on developing a CAD system for optimizing telecommunication systems. Since 1989 he has been with the University of Sydney where he is currently a reader in electrical engineering. His research interests include medical imaging, signal and image processing, computer vision, neural networks and pattern recognition. He is an author of more than 100 technical papers in these areas. Dr Yan is a senior member of IEEE, and a member of SPIE, International Neural Network Society (INNS), Pattern Recognition Society (PRS), and Society of Magnetic Resonance (SMR).